

**Supporting Information:**

**Fabrication of ultra-dense sub-10 nm in-plane Si nanowire arrays from a novel block copolymer method: optical properties**

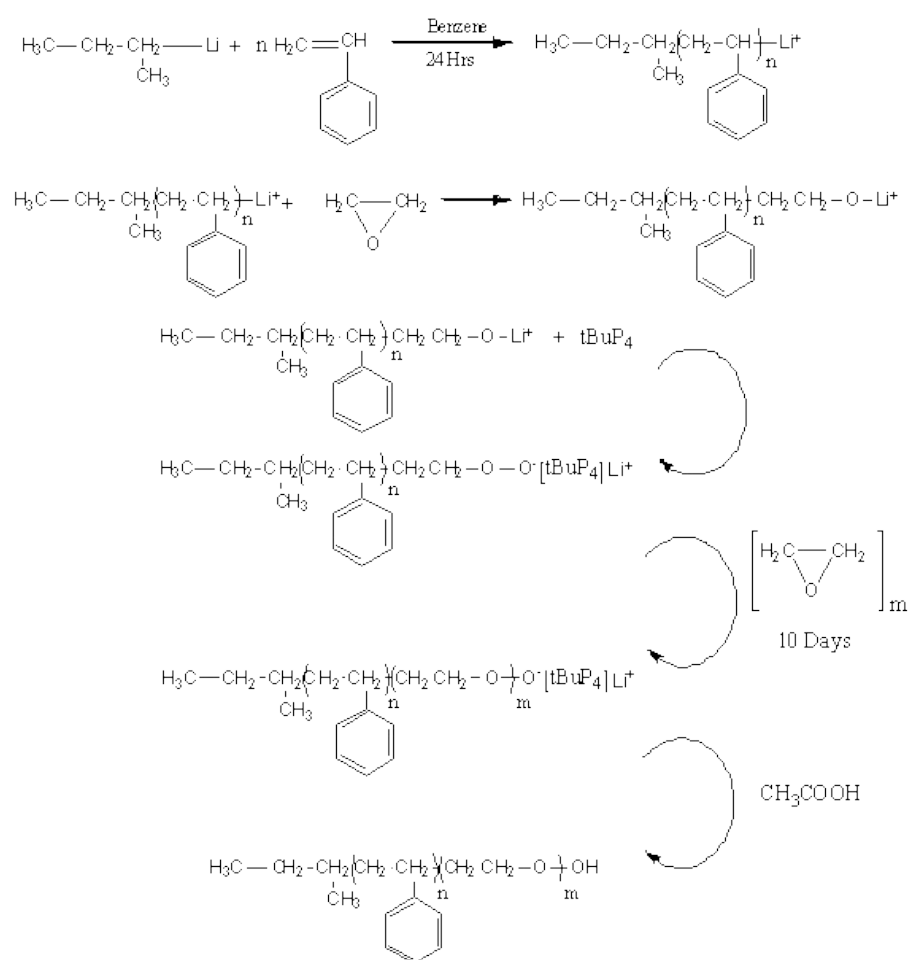
Tandra Ghoshal,\* Christos Ntaras, John O'Connell, Matthew T. Shaw, Justin D. Holmes, Apostolos Avgeropoulos, Michael A. Morris\*

**Synthesis and characterization of the synthesized PS-PEO:**

*Materials:* Ethylene oxide (all materials Sigma Aldrich unless stated) was dried over  $\text{CaH}_2$ , purified through  $n\text{-BuLi}$  twice for 30 min at  $-10^\circ\text{C}$  and was then distilled into an appropriately calibrated Pyrex ampule for use. Phosphazene base ( $\text{P}_4\text{-t-Bu}$ ) (1M solution in hexane),  $\text{sec-BuLi}$  (1.4 M solution in cyclohexane) and acetic acid (Panreac) were used without further purification. Benzene (Chem Lab, 99.7%) was freshly distilled from  $\text{CaH}_2$  and polystyryl lithium ( $\text{PS}^{(+)}\text{Li}^{(-)}$ ) and kept for further use. Styrene and dibutylmagnesium were purified through  $\text{CaH}_2$  distillation and added to calibrated Pyrex ampules. Various other solvents/salts were used as detailed toluene, Tetrahydrofuran (THF), anhydrous alcohol (ETH), Dimethylformamide (DMF) and Lithium chloride. Single crystal (100) boron doped (P type) silicon wafers with a native silica layer were used as general substrates. Different hard mask substrates such as Si-ARC (anti-reflective coating), alumina and carbon hard mask (CHM) etc. are selected to check the applicability of the pattern formation. For filtration, Fluoropore™ PTFE filter membranes with a pore size  $0.2\ \mu\text{m}$ , diameter of 25 mm thickness was used.

*Polymerization:* Styrene (2.5 g, 0.024 mol) was introduced from the Pyrex ampoule into a flask under high vacuum containing 200 mL of freshly distilled benzene. Approximately, 1 mmol of  $\text{sec-BuLi}$  (initiator) was added and the mixture was left to react for 24 hours at room temperature. Then, 2.5 g (0.057 mol) ethylene oxide was introduced in the mixture from a Pyrex ampule. The red solution due to active  $\text{PS}^{(-)}\text{Li}^{(+)}$  became transparent after the addition

of ethylene oxide. The reaction mixture was stirred for 2 h, followed by the addition of 0.80 mmol of  $P_4$ -t-Bu in order to improve the propagation reaction for the polymerization of ethylene oxide. The reaction mixture was stirred for 10 days at 40°C. It should be noted that in this approach we used benzene as solvent rather than tetrahydrofuran as it led to stricter control of the EO polymerization reaction presumably due to its' non-polar nature. The reaction was terminated with approximately 0.50 mL of acetic acid. In Scheme 1 represents the reactions for the synthesis of the diblock copolymer.



**Scheme 1** Reactions for the synthesis of the lamellar PS-PEO diblock copolymer.

*Characterizations:* GPC measurements were carried out with THF as eluent, using the PL GPC-50 (Polymer Laboratories) instrument at 40°C while the average molecular weight was determined with membrane osmometry using Osmomat 090 (Gonotec).  $^1\text{H}$ -NMR

experiments were performed in CDCl<sub>3</sub>, on a Bruker AVANCE II spectrometer at 250 MHz. The molecular characterization results for the synthesized BCP are given in Table S1 reveal lamellar phase system with the molecular weight (5.5k-5.3k).

<b>SAMPLE</b>	$\bar{M}_n(\text{PS})$ g/mol (SEC)	$I_{(\text{PS})}$ (SEC)	$\bar{M}_n(\text{total})$ g/mol (MO)	$\bar{M}_w(\text{total})$ g/mol (SEC)	$I_{(\text{total})}$ (SEC)	$f_{(\text{PS})}$ (SEC)	$f_{(\text{PS})}$ ( <sup>1</sup> H-NMR)
<b>PS-b-PEO</b>	<b>5500</b>	<b>1.05</b>	<b>10800</b>	<b>11550</b>	<b>1.07</b>	<b>0.51</b>	<b>0.52</b>

Table S1. Molecular characteristics of the PS-b-PEO.

In Fig. S1 the final GPC chromatograph is shown, indicating the very low polydispersity of the final diblock copolymer. <sup>1</sup>H-NMR experiments were performed in CDCl<sub>3</sub>, on a Bruker AVANCE II spectrometer at 250 MHz.

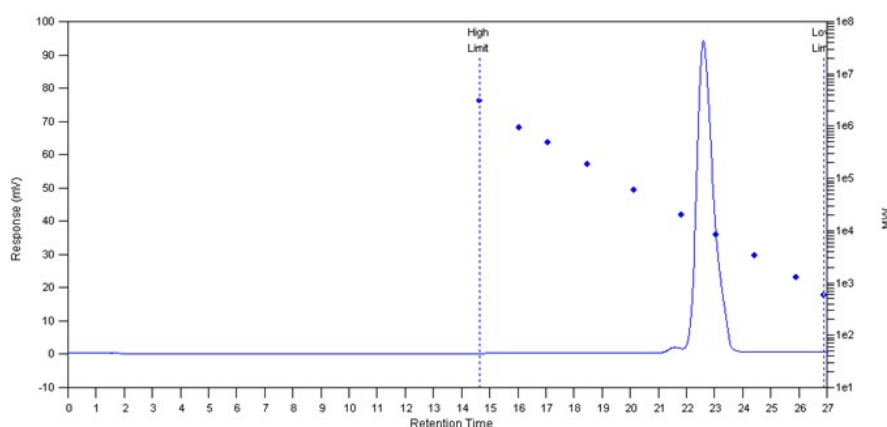


Fig. S1 SEC chromatograph of the final diblock PS-b-PEO.

<sup>1</sup>H-NMR spectra (Fig. S2) indicates shifts corresponding to  $\delta = 4.40 - 5.00$  (CH<sub>2</sub>O) for poly(ethylene oxide) segments and 6.80 - 7.50 (aromatic, C-H) for polystyrene respectively. The fact that the molecular characteristics from GPC and <sup>1</sup>H-NMR for the weight fraction are almost identical indicates molecular and compositional homogeneity.

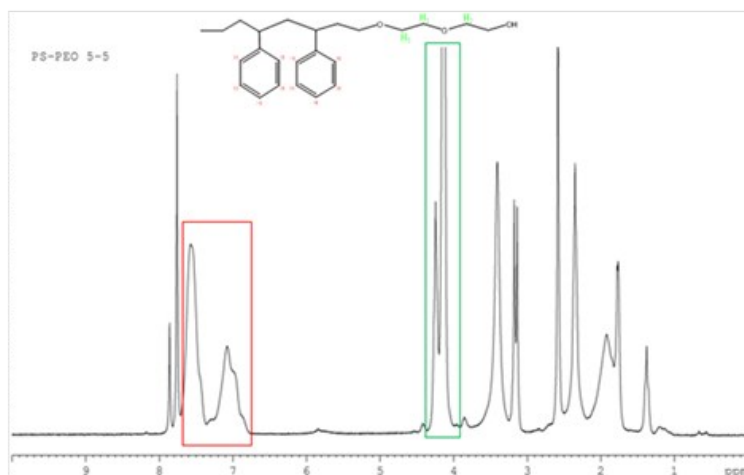


Fig. S2 <sup>1</sup>H-NMR spectra of sample PS-b-PEO indicating the chemical shifts of the four protons for PEO at ~4-4.5 ppm (green) and of the five aromatic protons for PS at ~6.8-7.5 ppm (red).

### Structural variation with film thickness:

Manipulation of the surface/interfacial energies is required to achieve the monolayer of perpendicular orientation of the lamellae depending on the interplay between the film thickness and the natural period.<sup>[1-3]</sup> For the PS-b-PEO system, the blocks exhibit asymmetric affinities for the solid substrate and the air interface where the hydrophilic PEO will preferentially wet the substrate surface (favourable PEO-substrate interactions) whilst PS will tend to segregate to a vacuum interface to form a PS-rich layer (PS has a lower surface energy,  $\gamma_{PS} = 33 \text{ mNm}^{-1}$ ;  $\gamma_{PEO} = 43 \text{ mNm}^{-1}$ ).<sup>[4]</sup> The film thickness was varied by changing the polymer-toluene concentrations from 0.5 L to 2 L in order to understand the self-assembly process, the orientation of the lamellae and the surface structural variation. No ordering is achieved for the film thickness below L (Fig. S3a). When the film thickness was increased to just above L (~ 17 nm), localized ordering with short stripes and plateaus without any ordering coexist (Fig. S3b and S3c). Long continuous stripes where lamellae oriented perpendicular to the substrate are realized over the substrate area for the thickness of ~ 1.5L (22 nm). Although local area defects in the form of small particulate or absence of patterns (below 25 nm<sup>2</sup> area) are observed, no large area dewetting or thickness undulation is evident.

Further thickness increment ( $> 22$  nm) results the coexistence of parallel (island) and perpendicular lamellae orientation. Longer continuous line-like patterns with perpendicular lamellar arrangements over  $2\text{-}4\text{ }\mu\text{m}$  area were formed with increasing film thickness to 30 nm (Fig. S3d). The film thickness used in this study is  $\sim 22$  nm to achieve a monolayer of the lamellae for the simplicity and ease in the fabrication of Si nanowires through the pattern transfer process. Note that the addition of Li ions at the centre of the film also contributes towards the thickness of the film.

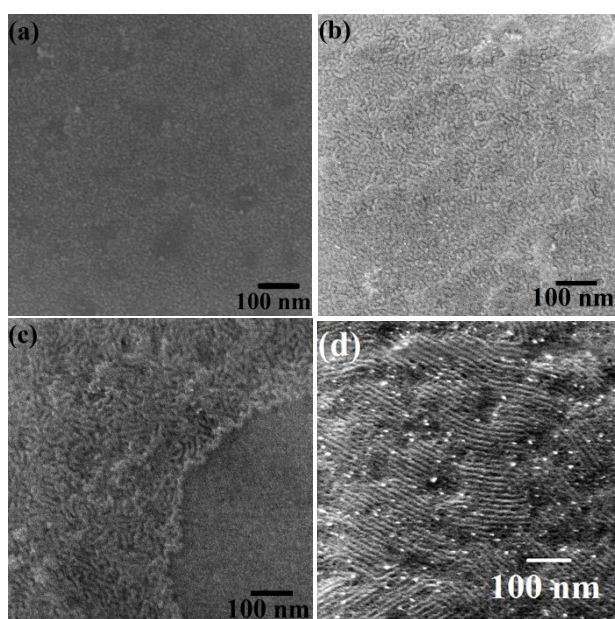


Fig. S3 SEM images of PS-b-PEO thin film after solvent annealing in toluene at  $60^{\circ}\text{C}$  for 30 min with the addition of 0.05 ml of LiCl-THF for the film thickness of (a) 10 nm (b and c) 17 nm and (d) 30 nm.

#### **Thermal stability of the nanowires:**

The nanowires formed using this inclusion technique is well-adhered to the substrate and thermally robust. Typical data are presented in the inset of Fig. S4 which shows iron oxide nanowires after air calcination at  $800^{\circ}\text{C}$  for 1 h, revealing their ordered structure in most of the areas of the substrate. The only effect of heating was a reduction in the average diameter and height consistent with high temperature densification as measured by SEM and

ellipsometry respectively. In the case of iron oxide nanowires on Si substrates, the diameters and heights were found to reduce by  $\sim 2$  nm for the air calcination at  $800^{\circ}\text{C}$  for 1 h presumably due to some sintering and, hence, densification. The average diameters of the nanowires were 6-7 nm with a lamellar spacing of 14-16 nm. The arrays of iron and nickel oxide nanowires on Si substrate were examined to be thermally stable upto  $1000^{\circ}\text{C}$  which depends on the material properties and the nature of the substrates.

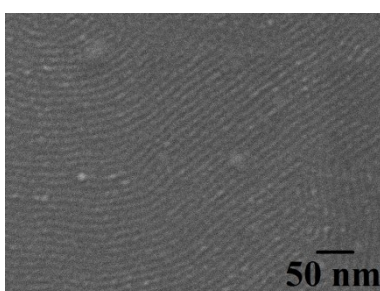


Fig. S4 Ordered iron oxide nanowire arrays after air calcination at  $800^{\circ}\text{C}$  for 1 h.

#### **Effects of precursor concentration:**

Figs. S5 (a) and (b) shows the surface morphology and topography of the films for different precursor concentrations of 3 and 5 wt% in 2-propanol stirred for 30 min respectively. Fig. S5a shows the nanowires are predominantly continuous but there is enhanced surface roughness, thickness variations and pattern degradation. Further, large scale surface roughness or thickness undulation across the surface was noticed. An excessive metal precursor concentration (Fig. S5b) results in oxide depositions all over the substrate area with few nanowires visible because of overloading of the precursors within the PEO block.

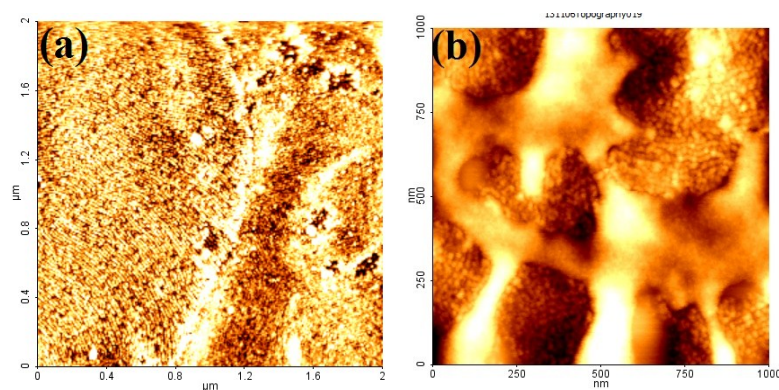


Fig. S5. Surface

morphology

and topography of the films for different precursor concentrations of (a) 3 and (b) 5 wt% in 2-propanol stirred for 30 min respectively.

### XPS analysis of iron oxide and nickel oxide nanowire arrays:

The Fe 2p core level spectrum (Fig. S6a) consists of two sharp peaks at 711.4/725.2 eV corresponding to the Fe 2p<sub>3/2</sub> and Fe 2p<sub>1/2</sub> signals for the iron oxide nanowire arrays following calcination at 800<sup>0</sup> C for 1h. A high binding energy satellite (+8 eV shift) can also be seen and these data are consistent with formation of Fe<sub>2</sub>O<sub>3</sub>.<sup>[5-6]</sup> A typical XPS survey spectrum (Fig. S6b) of iron oxide nanowires after annealing confirms the expected presence of Si, O, C and Fe. The C1s feature is relatively small and demonstrates effective removal of carbon species after annealing. Its intensity is consistent with adventitious material formed by adsorption and other contamination during sample preparation. Similar nature was observed from Ni 2p spectra for nickel oxide nanowire arrays which confirms both Ni<sup>+2</sup> and Ni<sup>+3</sup> in nickel (III) oxide (after UV/Ozone treatment) transformed to NiO, nickel (II) oxide after annealing shown in Figs. S6c and d.

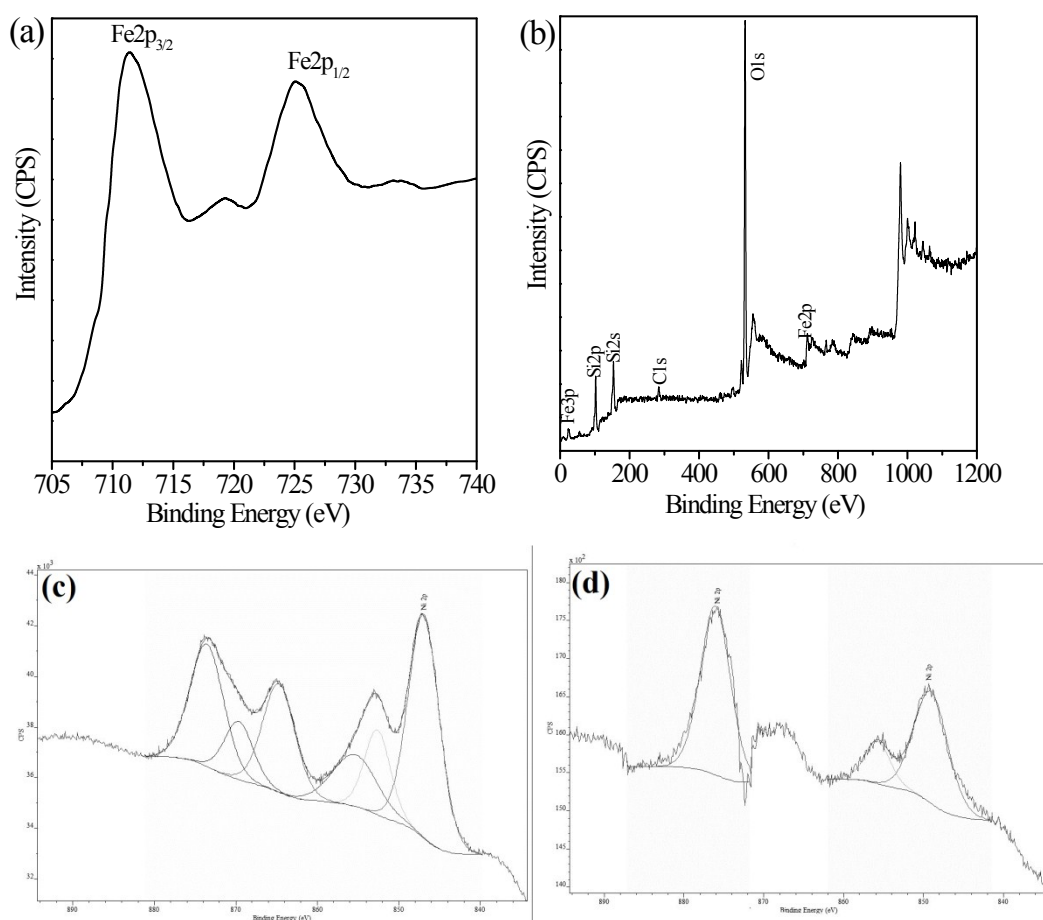




Fig. S6 (a) Fe 2p spectra and (b) survey spectra of iron oxide nanowire arrays following calcination at 800<sup>o</sup> C for 1h. Ni 2p spectra of nickel oxides nanowire arrays after (c) UV/Ozone treatment and (d) following calcination at 800<sup>o</sup> C for 1h.

**Effects of etching time and precursor concentrations on the pattern transfer onto Si:**

Fig. S7a shows the large area SEM image of the substrate after 2 min Si etch for the iron oxide nanowire arrays prepared with 1.8 wt% precursor-2 propanol solution. The contrast enhancement shows pattern transfer occurred but discontinuous nanowires were noticed in few places.

Fig. S7b-d shows the SEM images of the substrate after 1 min Si etch using the iron oxide prepared with 1.6 wt%, 2 wt% and 3 wt% of precursor. Identical ordered nanowire patterns obtained after pattern transfer for all the films. Almost no pattern transfer is realized for the highest precursor concentration (Fig. S7d).

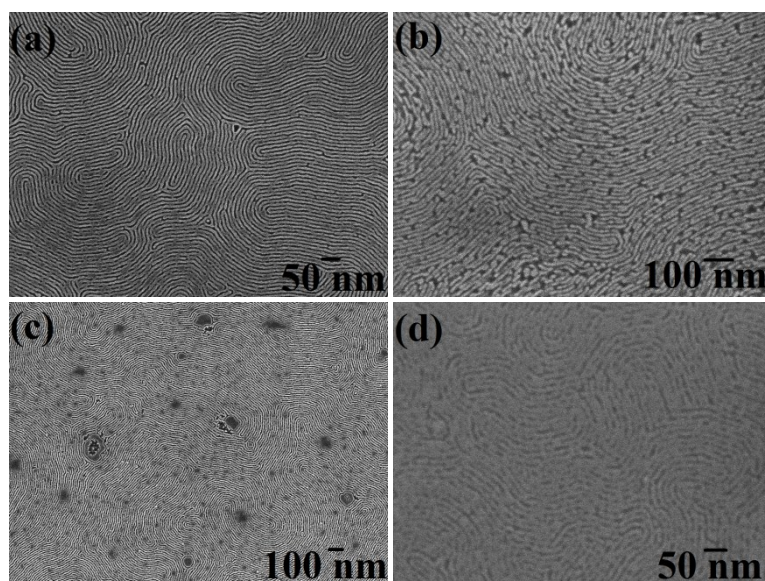


Fig. S7. (a) SEM image pattern transferred substrate using iron oxide nanowire arrays prepared with 1.8 wt% precursor-2 propanol solution after 2 min Si etch. SEM images of the pattern transferred substrate after 1 min Si etch using iron oxide prepared with (b) 1.6 wt%, (c) 2 wt% and (d) 3 wt% of precursor concentrations.



- [1] J. G. Kennemur, L. Yao, F. S. Bates, M. A. Hillmyer, *Macromolecules*, **2014**, *47*, 1411.
- [2] A. Nunns, J. Gwyther, I. Manners, *Polymer*, **2013**, *54*, 1269.
- [3] M. Ceresoli, F. F. Lupi, G. Seguini, K. Sparnacci, V. Gianotti, D. Antonioli, M. Laus, L. Boarino, M. Perego, *Nanotechnology*, **2014**, *25*.
- [4] T. Ghoshal, M. T. Shaw, C. T. Bolger, J. D. Holmes, M. A. Morris, *J. Mater. Chem.*, **2012**, *22*, 12083.
- [5] P. Mills, J. L. Sullivan, *J. Phys. D-Appl. Phys.*, **1983**, *16*, 723.
- [6] T. Fujii, F. M. F. de Groot, G. A. Sawatzky, F. C. Voogt, T. Hibma, K. Okada, *Physical Review B*, **1999**, *59*, 3195.